Virchows Archiv A Pathol Anat (1990) 417:279–290

Virchows Archiv A
Pathological Anatomy and Histopathology

Sequential ultrastructural podocytic lesions and development of proteinuria in serum sickness nephritis in the rat*

Hui-Jun Duan

Department of Pathology, Shinshu University School of Medicine, 3-1-1 Asahi Matsumoto, Nagano 390, Japan

Received January 29, 1990 / Accepted February 26, 1990

Summary. Serum sickness nephritis was induced in Fisher rats by immunization with egg albumin (EA) and correlations between immune complex deposition, alterations of podocytes and development of proteinuria were analysed. Immunoelectron microscopy showed that EA, rat IgG and C3 were confined to the electron-dense deposits (Ds). From 3 weeks, when significant proteinuria had developed, the subepithelial region was filled with large numbers of Ds on the peripheral capillary wall as well as in the paramesangium. The loss of slit diaphragms and detachment of foot processes overlying Ds were observed and the escape of Ds into urinary space was frequently detected. Morphometric evaluation showed that the volume of subepithelial Ds and the number of the sites of podocytic detachment correlate significantly with the amount of proteinuria. In addition, the native ferritin injected via the abdominal aorta was seen in large amounts in the urinary space near the areas devoid of epithelial covering. The development of podocytic detachment was clearly coincident with the appearance of proteins with a larger molecular weight in urine. From these results, it is suggested that the loss of slit diaphragms and the detachment of podocytes resulting from the progressive accumulation of Ds will allow the leakage of proteins of larger molecular weight across the capillary wall. These podocytic lesions may be one of the main aetiologies for the development of heavy proteinuria in this model.

Key words: Serum sickness nephritis – Proteinuria – Immune complex – Podocyte detachment – Slit diaphragm

Introduction

In immune-complex-mediated glomerulonephritis glomerular tissue injury is evoked in association with the localization or accumulation of immune complexes in the glomeruli (McCluskey 1983; Fries et al. 1988). It is therefore important to clarify the relationship between immune complex formation and the lesions of the glomeruli as well as the development of proteinuria, the most important sign of glomerulonephritis. It has been found that subepithelial immune complex formation results in the injury of the glomerulus and the appearance of proteinuria (Schneeberger et al. 1979; Adler et al. 1983). In contrast, immune complex deposition on the endothelial layer or in the lamina rara interna does not initiate proteinuria (Fries et al. 1988; Sawtell et al. 1988). These results suggest that the site of glomerular immune complex accumulation is an important factor in determining glomerular lesions with proteinuria.

The alterations of podocytes in relation to proteinuria have been extensively examined in aminonucleoside nephrosis (Venkatachalam et al. 1970; Ryan and Karnovsky 1975; Ryan et al. 1975a, b, 1978; Caulfield et al. 1976; Kanwar and Rosenzweig 1982; Messina et al. 1987). The detachment of podocytes from the glomerular basement membrane (GBM), partial or complete, has been described as coinciding precisely with the onset of proteinuria and as a primary site of GBM in protein leakage (Ryan and Karnovsky 1975; Ryan et al. 1978; Kanwar and Rosenzweig 1982; Messina et al. 1987). The process of detachment of podocytes has also been observed in some models of immune complex nephropathy (Schneeberger et al. 1979; Adler et al. 1983).

Serum sickness nephritis is characterized by the marked deposition of immune complex, not only in mesangium but also in the subepithelial region. However, the relationship between immune complex accumulation and the alterations of podocytes as well as the development of proteinuria is as yet unclear. In this study, I have analysed the sequence of events of immune deposition and the lesions of podocytes, especially podocytic detachment, in relation to proteinuria in this model.

Materials and methods

Serum sickness nephritis was induced in 10-week-old male -F344/JCL rats as previously described (Shigematsu and Koyama 1988a–c). The experimental procedures are summarized in Fig. 1.

* Part of this study was presented at the 78th Annual Meeting of Japan Pathological Society, in Kyoto, March 1989

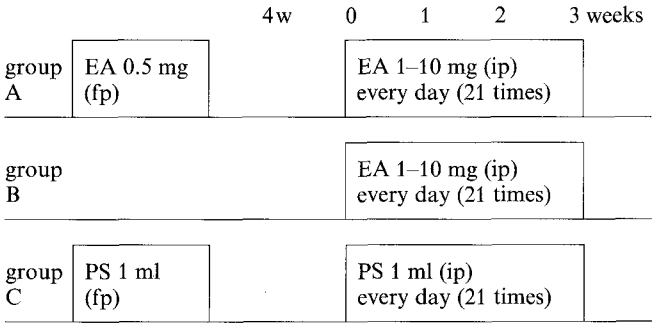

Fig. 1. Experimental protocol: preimmunization with egg albumin (*EA*) was performed in the foot pads (*fp*). Intraperitoneal (*ip*) administration of EA was started 4 weeks after the preimmunization for 3 weeks. No preimmunization was given in group B. Physiological saline (*PS*) was injected in group C instead of *EA*

In group A 40 rats were preimmunized by injection with 0.5 mg egg albumin (EA) with Freund's complete adjuvant into the foot pads. After a 4-week interval, each rat was then injected intraperitoneally (i.p.) with increasing amounts of EA for 21 days (1 mg on the 1st day, 2 mg on the 2nd day, 5 mg on the 3rd and 4th days, and 10 mg for the last 17 days).

In group B 20 rats were used. No preimmunization with EA was performed and only i.p. injection of EA was done in a similar manner to that in group A for 21 days.

In group C 20 rats were used. Instead of EA, physiological saline (PS) was injected into foot pads and peritoneal cavity, as in group A.

The urinary samples were collected daily from 2 to 3 weeks after the beginning of i.p. administrations and weekly after that, and on the day before killing. The 24-h urinary protein excretion was measured by the sulphosalicylic acid method.

At the time of death, each nephrotic and control animal was anaesthetized i.p. with sodium pentobarbital, and the kidneys were fixed in situ by perfusion of periodate-lysine-paraformaldehyde (PLP, pH 7.4) from the abdominal aorta.

For light microscopy, kidneys, liver, spleen and lungs obtained were fixed in 10% buffered formalin solution (pH 7.4), embedded in paraffin, sliced into thin sections, and used for routine microscopic examination. For immunofluorescence, part of renal contex was snap-frozen in *n*-hexane (−70° C) and cut in a cryostat (Ames, Miles Lab., Ill., Tokyo, Japan). FITC-conjugated antisera, rabbit anti-chicken egg albumin, anti-rat IgG, and C3 were obtained commercially (Cappel Laboratories, Malvern, USA), and used for direct immunofluorescent microscopy. The antisera were used at a dilution of 1:20, and incubation with antisera was for 60 min at room temperature.

Electron microscopy was carried out on renal tissues fixed in 2.5% glutaraldehyde (pH 7.6), postfixed by 1% osmic acid, and embedded in Quetol 812. Ultrathin sections were stained with uranyl acetate and lead citrate, and were examined by HS-9 or HU-11A electron microscope. Tissue for immunoelectron microscopy was fixed in PLP (pH 7.4), postfixed by 2% osmic acid, and embedded in Quetol 812. Ultrathin sections were obtained.

Immunocytochemical labelling was performed according to the methods of Bendayan and Zollinger (1983) and Hearn et al. (1985). Ultrathin sections were picked up on nickel grids and placed in a drop of 4% solution of sodium metaperiodate for 1 h. Grids were further treated for 1 h with 0.1 mg/ml bovine serum albumin (BSA) in phosphate-buffered saline (PBS) and washed for 10 s in a drop of PBS. The grids were incubated with rabbit anti-EA antisera, anti-rat IgG and anti-rat C3 (Cappel Laboratories) at room temperature for 1 h. After being washed with PBS, the grids were then incubated with protein A-colloidal gold (E. Y. Labs, Biochemical Division, San Mateo, Calif.) diluted 1:40 with PBS for 1 h. Grids were again washed for 10 s with PBS and finally for 10 s with distilled, filtered water. The sections labelled with colloidal gold were stained with uranyl acetate and lead citrate and examined by HS-9 electron microscope.

Twenty rats of group A from five different stages when protein excretion was differed statistically were used to assess the volume of mesangial and subepithelial electron-dense deposits (Ds). Photographs (16–20 sheets in each glomerulus) from two glomeruli were taken in each rat kidney specimen (initial magnification was ×2000, printing at a final magnification of ×4000). The mesangial and subepithelial Ds and glomeruli were outlined, and the volume was estimated by digigrammer system (model-G series, Mutoh). These photographs were also used to assess the number of balloon-like vacuoles in podocytes. The vacuoles larger than 1 cm in diameter at a magnification of ×4000 and with attenuated epithelial covering were taken as balloon-like vacuoles.

Twelve rats from three different stages were used to assess the site of epithelial detachment. Five glomeruli were examined in sections of kidneys from each rat and the total number of the sites of epithelial detachment found in five glomeruli of each rat was analysed.

To estimate the change of size barrier of the GBM during the course of immune complex deposition additional studies were performed. The urinary protein fraction was determined on urine samples of 20 rats by sodium dodecyl sulphate polyacrylamide gel electrophoresis (SDS-PAGE). SDS-PAGE electrophoresis was performed on 12% slab gels according to the method reported in the literature (Laemmli 1970; Fraij 1989). The urine samples were normalized to a protein concentration of 180–200 mg/dl by dilution with water or by concentration with a minicon B concentrator (Amicon, Grace Japan Company). A 10 µl aliquot of urine was mixed with an equal volume of double-strength Laemmli buffer containing SDS and 5% 2-mercaptoethanol. The mixture was boiled for 5 min and centrifuged at 16,000 *g* for 1 min. A 10 µl aliquot of supernatant fluid was applied to each well of the gel. The molecular mass markers were dissolved and processed in the same manner as urine specimens. Electrophoresis was performed at room temperature, at a constant voltage of 200 V for 2.5 h. Gels were stained, destained and dried. After drying laser scanning was performed with densitometer (Helana Institute).

Tracer study with native ferritin was also performed. Six control and six proteinuric rats were used for in vivo tracing with native ferritin. The native ferritin was perfused as previously described (Kelley and Cavallo 1977, 1978, 1980). The abdominal cavity was opened and a 22-gauge needle was introduced into the aorta below the origin of the renal arteries. A ligature was placed above the origin of the left renal artery so as to permit all of the perfusate to flow into left kidney. The PBS was first perfused for 2–5 min to wash the kidney free of blood, then native ferritin (2 mg/g body weight; United States Biochemical Corporation, Ohio) in PBS (30 mg/ml) was perfused into the aorta over 15 min. A renal biopsy was taken. The kidney was fixed by perfusion of 4% paraformaldehyde before the rat was sacrificed. The samples were routinely processed for electron microscopy. The thin sections were unstained or stained only with lead citrate and examined by HS-9 electron microscope.

Results

The time hereafter refers to the time from the beginning of intraperitoneal administration of EA, throughout the results.

The urinary protein excretion never exceeded 20 mg/24 h in the control rats to which PS was injected instead of EA. This low rate remained until day 16 in the experimental rats. In most the onset of proteinuria was detected on approximately day 17–19 with values ranging from 26 to 45 mg/24 h. These rose quickly and reached over 100 mg/24 h in 1–3 days after the onset. The maxi-

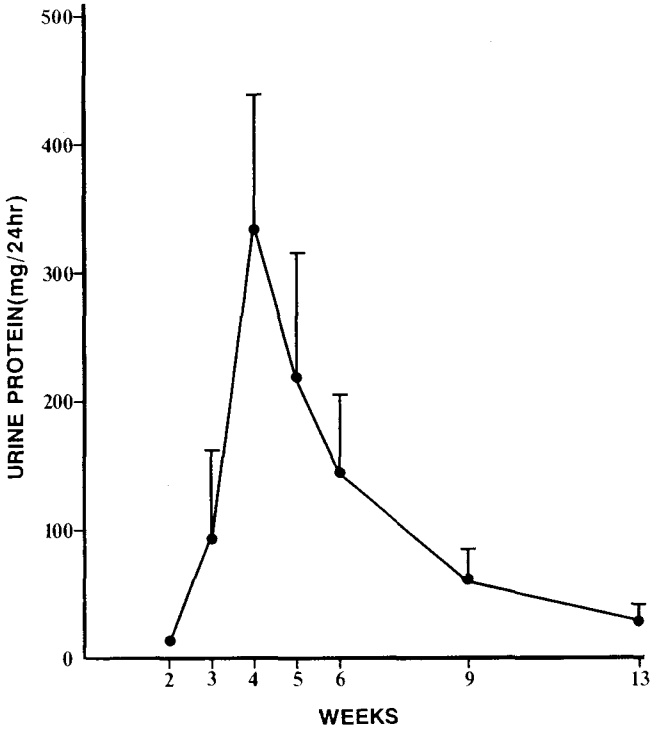

Fig. 2. Twenty-four-hour urine protein measured by sulphosalicylic acid technique, from 2 weeks to 3 months following intraperitoneal injection of EA. Values are mean ± standard error of the mean

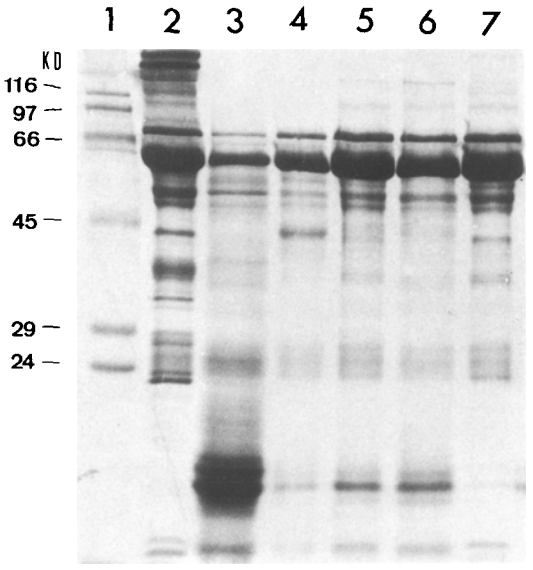

Fig. 3. SDS-PAGE patterns of urinary proteins at various stages of serum sickness nephritis.
1 Molecular weight markers; *116 kDa* (galactosidase); *94 kDa* (phosphorylase b); *66 kDa* (albumin, bovine); *45 kDa* (albumin, EGG); *29 kDa* (carbonic anhydrase); *24 kDa* (trypsinogen)
2 Rat serum
3 Urine sample of normal rat
4 Urine sample of rat with 40 mg/24 h of urine protein at 18 days
5 Urine sample of rat with 120 mg/24 h of urine protein at 3 weeks
6 Urine sample of rat with 200 mg/24 h of urine protein at 4 weeks
7 Urine sample of rat with 320 mg/24 h of urine protein at 4 weeks

Table 1. Urinary protein excretion, volume of subepithelial and mesangial Ds, number of the sites of detachment and balloon-like vacuoles of podocytes in animals killed at various times

Times of sacrifice	Urinary protein excretion[a]	Volume of mesangial Ds[b]	Volume of subepithelial Ds[b]	Number of podocytic detachments[c]	Number of balloon-like vacuoles[d]
2 weeks	8.5± 2.5	1.77±0.21	0.03±0.01		3.0± 1.2
17–19 days	36.0± 6.8	2.07±0.18	0.40±0.06		10.8± 3.8
3 weeks	116.5±14.8	2.36±0.47	1.18±0.19	10.5±3.8	18.3±12.1
4 weeks	324.5±12.5	1.87±0.53	1.41±0.18	25.0±5.4	26.5±11.9
6 weeks	113.5±23.3	1.83±0.10	0.55±0.15	13.5±2.1	10.5± 2.1

[a] The values are the mean ± SE of four animals in each stage, mg/24 h
[b] The values are the mean ± SE of eight glomeruli from four animals in each stage, assessed from percentage of areas of mesangial and subepithelial Ds to that of glomerulus
[c] The values are the mean ± SE of four animals in each stage, calculated from the total number of five glomeruli in each animal
[d] The values are the mean ± SE of eight glomeruli from four animals in each stage

Ds, electron-dense deposits

mal values of protein excretion were found at 4 weeks (over 300 mg/24 h). Proteinuria then reduced and returned toward almost normal level by 3 months (Fig. 2). The severity of proteinuria and the rate of recovery between different animals varied. The urinary protein excretion rates of the experimental rats killed on different stages are significantly different (Table 1).

Two rats without preimmunization showed transient slight proteinuria (22 and 31 mg/24 h) at 4–5 weeks, but after that period urinary protein returned to below 20 mg/24 h.

As shown in Fig. 3, the proteins with a molecular weight smaller than 24000 daltons predominated in the urine samples of control rats and the urine samples of experimental rats collected before the onset of proteinuria. The urine samples collected on the day of onset of proteinuria showed mainly proteins with a molecular weight of 45000–66000 daltons. No protein with a mo-

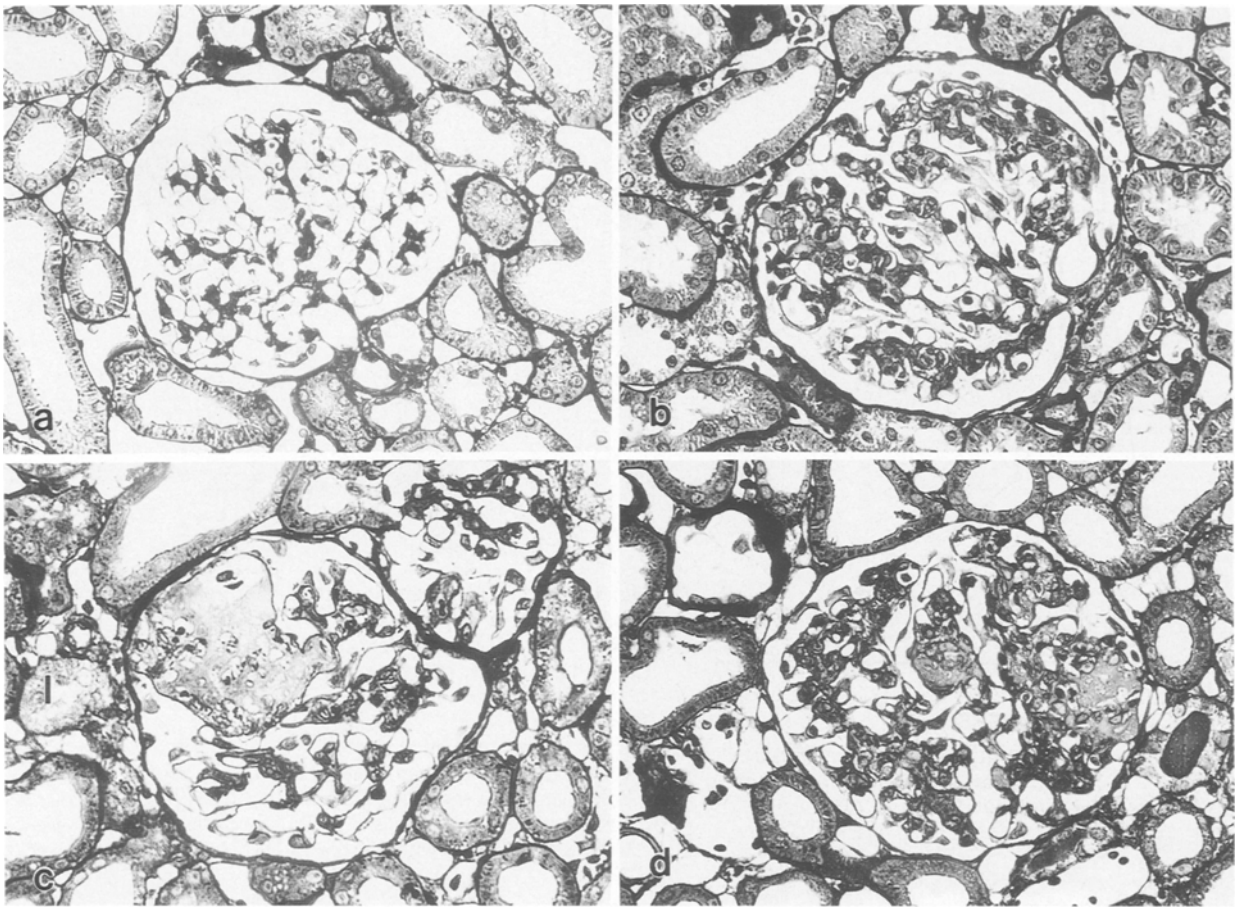

Fig. 4a–d. Light micrographs of glomeruli from rats at different stages: **a** mild mesangial expansion at 2 weeks; **b** hypercellularity at 18 days; **c** mesangiolysis at 3 weeks; **d** segmental sclerosis and adhesion of capillary loop with Bowman's capsule at 4 weeks. PAM, ×210

lecular weight larger than 97000 was detected. In the urine samples of rats with significant proteinuria, the proteins with a molecular weight larger than 97000 were clearly found and the amount of them was increased with the rise of urinary protein excretion rates.

On light microscopy at 2 weeks, glomeruli of group A rats exhibited mild mesangial widening (Fig. 4a), accompanied by increased number of mononuclear cells at 18 days (Fig. 4b). At 3 weeks, mesangiolysis was observed in focal and segmental distribution (Fig. 4c). Segmental sclerosis of glomeruli and adhesions of capillary loops with Bowman's capsule were occasionally seen at 4 weeks (Fig. 4d). In the rats of group B mild mesangial widening was found and no significant changes could be seen in group C.

From 2 weeks, the glomeruli of the group A rats showed strongly positive staining for EA, rat IgG and C3, with a diffusely granular pattern in mesangium and along the capillary walls. A weak positive staining in the rats of group B and a negative staining in the rats of group C were seen for EA, rat IgG and C3 respectively.

Using the immunogold method, accumulated gold particles for EA were localized to the mesangial and subepithelial Ds (Fig. 5a) and minimal dispersed gold staining was seen in the areas without Ds. Gold particles for IgG (Fig. 5b) and C3 (Fig. 5c) were distributed in a similar pattern to that of EA. The distribution of the gold particles was slightly uneven and the number of gold particles in Ds of higher density was increased more than that in the Ds with lower density. The density of Ds was gradually increased in 3 weeks in the mesangial area or 4 weeks in the subepithelial region. Before 3 weeks the subepithelial Ds contained smaller amounts of gold particles, where the density of Ds was lower than that of mesangial Ds. From 4 weeks, this difference in distribution of gold particles disappeared.

In the group A rats, mesangial dense deposits (MDs) were detected as early as 1 week. At 2 weeks the number of MDs was increased. By 3 weeks the volume of MDs reached the peak values seen throughout the experiment, but statistically, correlation between the changes of the volume of MDs and the amount of proteinuria could not be detected ($P \geqq 0.05$, Table 1). In contrast, the appearance of subepithelial dense deposits (PDs) was detected as late as 2 weeks and at this stage the PDs were small and infrequent. Usually, localization was limited within the lamina rara externa (Fig. 6a). The rats killed on days 17–19 at the time of the onset of proteinuria showed significant numbers of PDs (Fig. 6b). From 3 weeks, when significant proteinuria appeared, subepithelial regions of the capillary wall and paramesangium

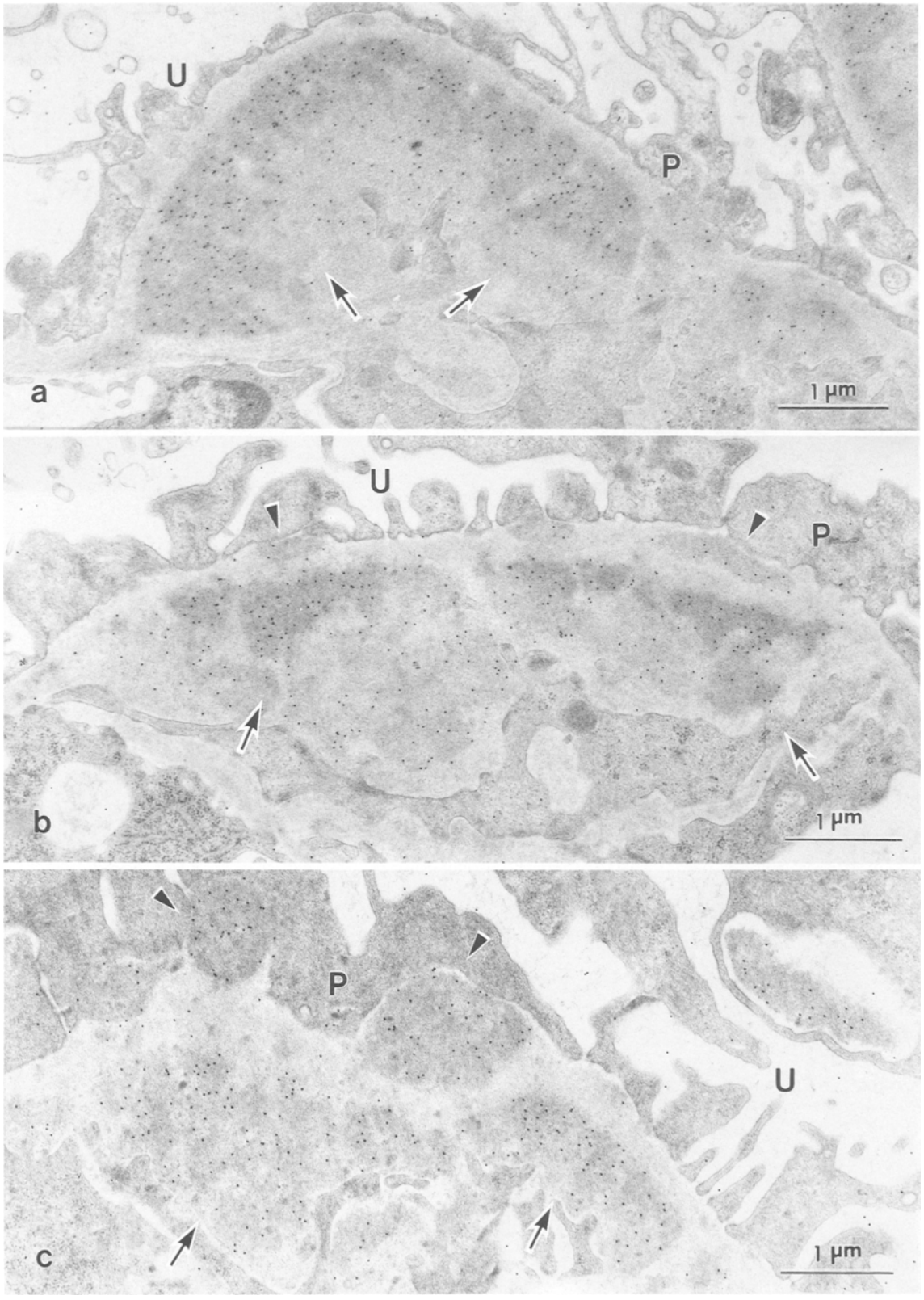

Fig. 5a–c. Immunoelectron micrographs of glomeruli from group A rats to show the localization of EA (**a**), IgG (**b**) and C3 (**c**) within mesangial (*arrow*) and subepithelial (*arrowhead*) electron-dense deposits. *U*, Urinary space; *P*, podocyte. ×18000

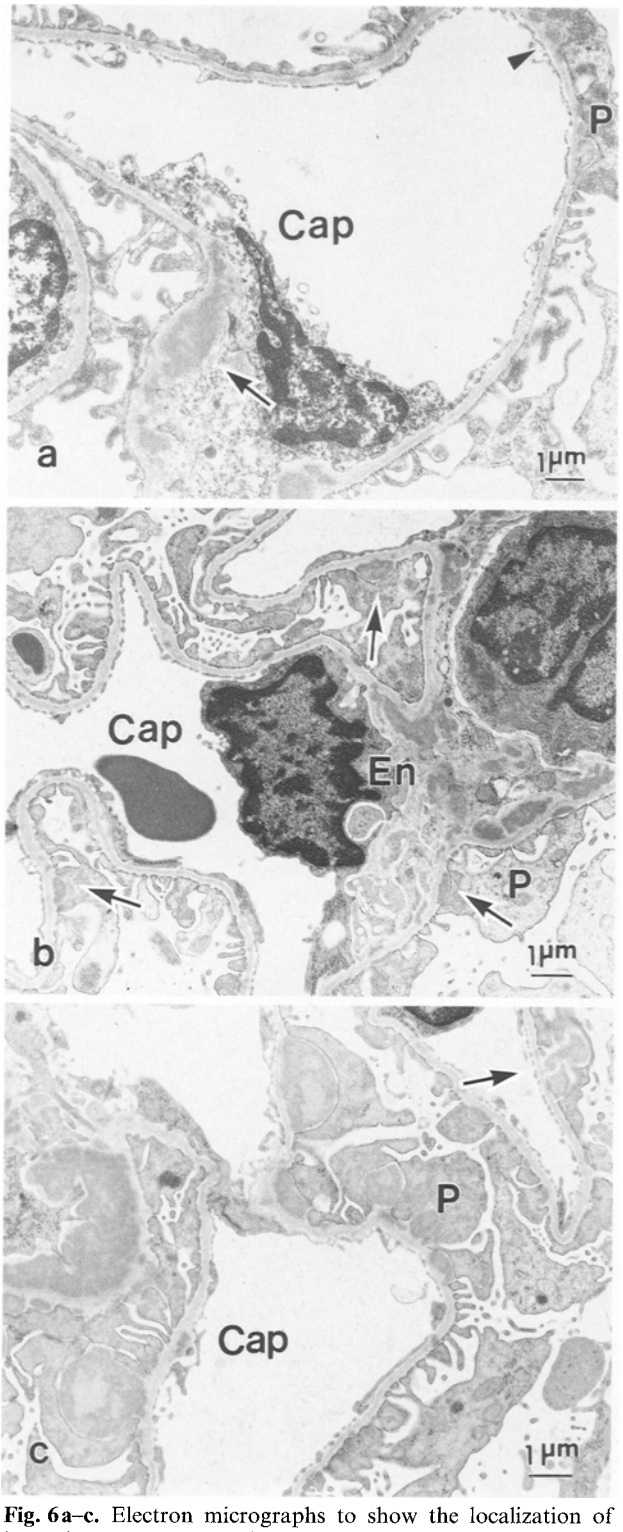

Fig. 6a–c. Electron micrographs to show the localization of Ds in various stages *P*, podocyte; *En*, endothelium; *Cap*, capillary lumen. **a** At 2 weeks, there are numerous electron-dense deposits present in the mesangium (*arrow*), but electron-dense deposits present in the subepithelial side are infrequent and small (*arrowhead*). × 5400. **b** At the time of onset of proteinuria, some of large electron-dense deposits also appeared in the subepithelial zone (*arrow*). × 5400. **c** At 3 weeks, there are numerous electron-dense deposits with various shape observed in subepithelial zone, one of which seems to pass into the subepithelial pocket across the epithelial defect (*arrow*). × 5400

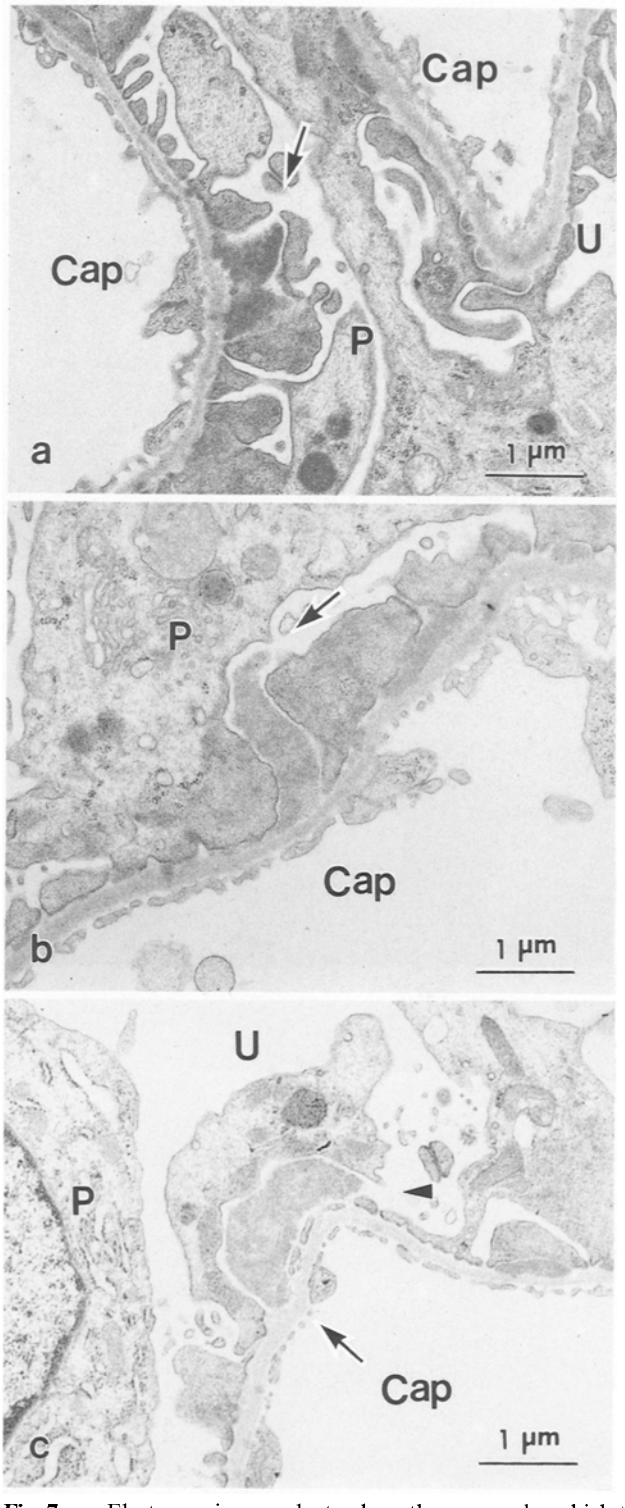

Fig. 7a–c. Electron micrographs to show the process by which the electron-dense deposits escape into subepithelial pocket in peripheral capillary wall. *U*, Urinary space; *P*, podocyte; *Cap*, capillary lumen. **a** The slit space is widened and the slit diaphragm is absent (*arrow*). × 13000. **b** The slit position is markedly lifted and widened. The slit diaphragm is not detected (*arrow*). × 13000. **c** The electron-dense deposits pass into the subepithelial pocket across the defect of the slit diaphragm (*arrow*), communicating with the urinary space (*arrowhead*). × 13000

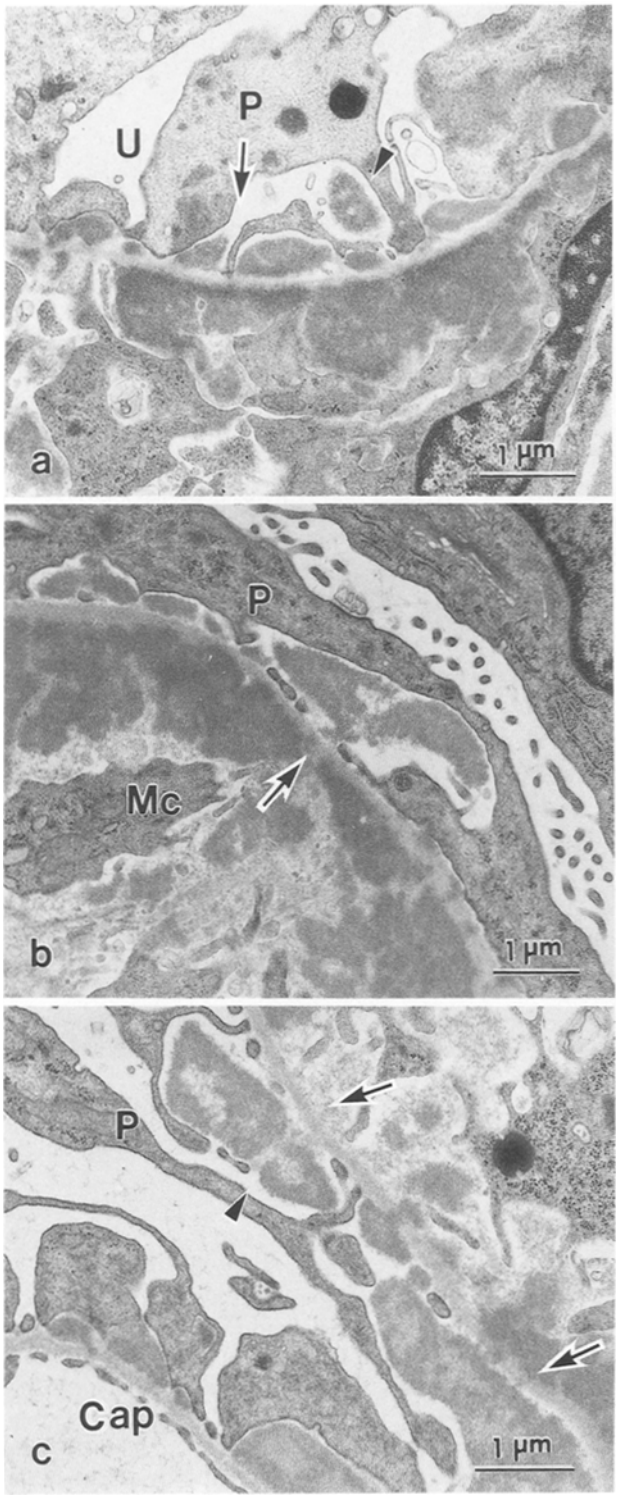

Fig. 8a–c. Electron micrographs showing the process by which the electron-dense deposits pass into a subepithelial pocket on paramesangium. *U*, Urinary space; *P*, podocyte; *Cap*, capillary lumen; *Mc*, mesangial cell. **a** The loss of slit diaphragms and the widening of slits are apparent (*arrow*) and electron-dense deposits are present in the subepithelial pocket (*arrowhead*). ×13000. **b** electron-dense deposits pass into the subepithelial pocket across the slit diaphragm; the continuity of electron-dense deposits can be seen (*arrow*). ×11500. **c** The podocyte overlying electron-dense deposits situated in the subepithelial pocket is lifted, leading to exposure of electron-dense deposits to the urinary space (*arrow*). ×13000

were filled with large numbers of PDs of various shapes, some of which were located beyond the slit pores (Fig. 6c). Morphometric evaluation indicated that the rats with higher proteinuria had significantly more PDs than those with lower proteinuria ($P \leqq 0.01$, Table 1).

Accumulation of deposits in subepithelial regions was sometimes associated with widening of the slit pores, loss of slit diaphragms and detachment of podocytes from GBM. Figure 7 shows the sequential changes in the peripheral capillary wall. Definite podocytic detachment could not be detected at 17–19 days, but some of the slits overlying the PDs apparently widened and the slit diaphragms were indiscernible (Fig. 7a). From 3 weeks, the widening of slits and the loss of slit diaphragms were much more apparent (Fig. 7b). The underlying PDs were seen escaping into subepithelial pockets across the defect, sometimes communicating with the urinary space (Fig. 7c).

In the paramesangium, similar changes were apparent. Sequential alterations, namely, the loss of slit diaphragms (Fig. 8a), escaping of PDs into subepithelial pockets (Fig. 8b) and the disappearance of podocytic cytoplasm overlying the materials in subepithelial pockets (Fig. 8c) were clearly observed.

In some areas where slit diaphragms had disappeared, the PDs were directly exposed to (Fig. 9a) or escaped into (Fig. 9b) the urinary space. Sometimes, continuity of PDs between urinary space and subepithelial region could be seen (Fig. 9c, d).

The foot processes in the areas with PDs were frequently flattened. In the areas where large PDs were present, flattened foot processes overlying the PDs were sometimes lifted and a wide gap was seen between the PDs and podocytic cytoplasm, forming a subepithelial pocket without direct communication with the urinary space (Fig. 10a, b). In some of these areas, podocytic cytoplasm was variously disrupted and the materials in the pocket were in direct communication with the urinary space (Fig. 10c).

Such podocytic detachment by accumulating PDs was clearly observed at 3 weeks, when significant proteinuria appeared, and showed a maximal value at 4 weeks. The differences between the number of the sites of podocytic detachment at 3 and 4 ($P \leqq 0.01$), 4 and 6 ($P \leqq 0.05$) weeks are statistically significant (Table 1).

Ferritin particles were largely confined to the lamina rara interna of the GBM in control rats. In proteinuric rats, they were seen throughout the width of the GBM, but were hardly seen in the urinary space in the areas with intact podocytes. However, they crossed the GBM and entered into the subepithelial pockets (Fig. 11a) or urinary space (Fig. 11b) near the areas where podocytes had detached from the GBM.

Other findings included the balloon-like vacuoles of the podocytes which were first found at 2 weeks. They increased in both number and size as proteinuria developed, and showed a maximal value at 4 weeks (Table 1). In the rats of group B a few small MDs were seen at 3 or 4 weeks, but no PDs were found. There were no Ds located in the urinary space. In the rats of group

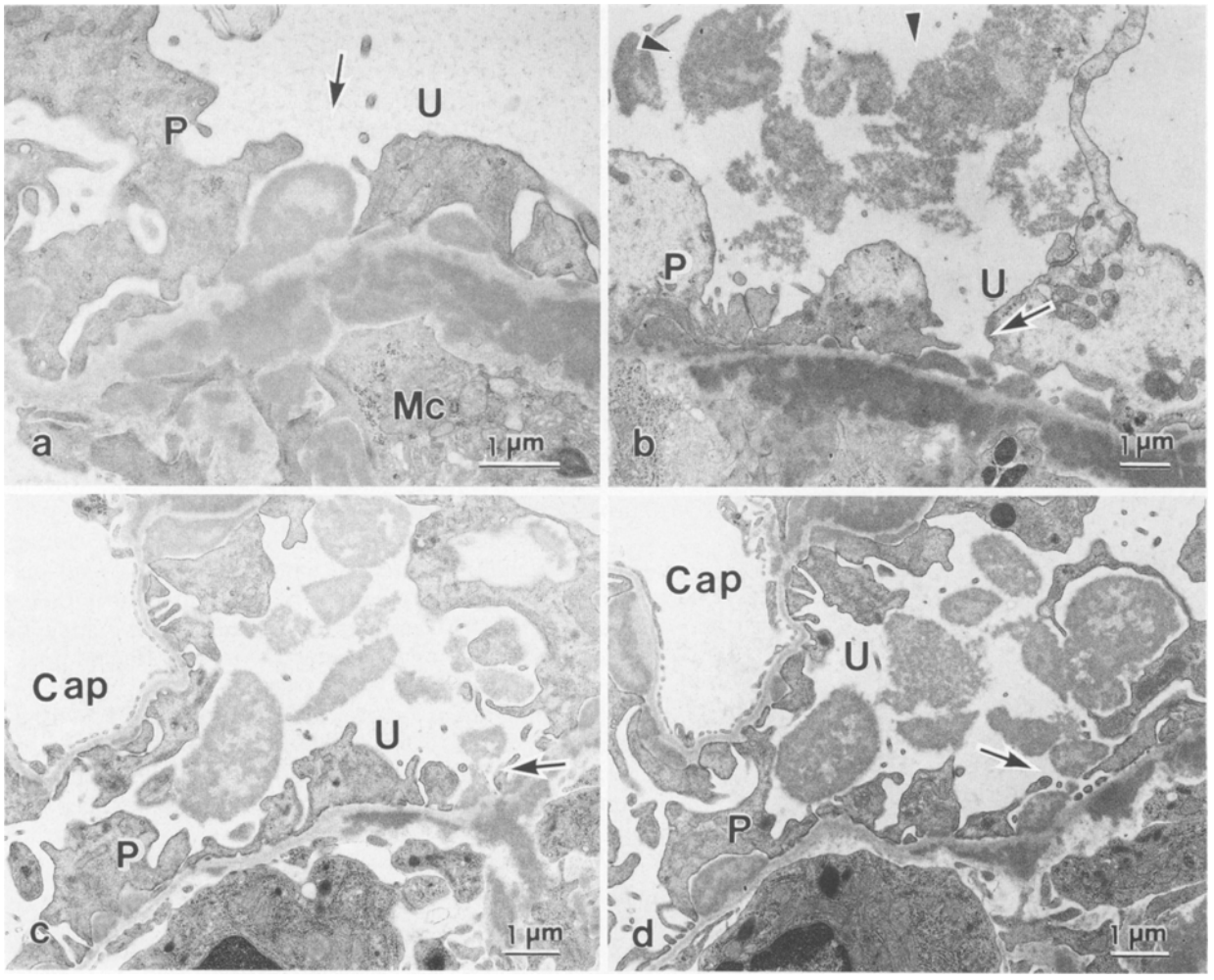

Fig. 9a–d. Electron micrographs to show the process by which the electron-dense deposits situated underneath the slit diaphragm mass directly into the urinary space. *U*, Urinary space; *P*, podocyte; *Cap*, capillary lumen; *Mc*, mesangial cell. **a** The slit diaphragm overlying the large electron-dense deposits is lacking at the tip of the electron-dense deposits, and electron-dense deposits is directly exposed to the urinary space (*arrow*). ×10750. **b** The loss of slit diaphragms and the widening of slits are apparent (*arrow*) and there are materials seemingly originating from electron-dense deposits in the urinary space (*arrowhead*). ×6500. **c, d** Serial sections of the same glomerulus. The electron-dense deposits are escaping into the urinary space across the defect of the slit diaphragm. The continuity between the urinary space and the subepithelial region following the the loss of epithelial covering can be seen (*arrow*). ×7500

C, no deposits were seen in the glomeruli. The detachment and balloon-like vacuoles of podocytes could not be detected in groups B and C.

The effacement of foot processes and microvilli formation appeared early and was followed by proteinuria. These changes were also seen in group B rats without preimmunization. No marked increase in these changes could be seen in rats with massive proteinuria. The alterations do not seem to correlate with the amount of proteinuria.

Discussion

The deposition of antigen EA, rat IgG and C3 has previously been observed by immunofluorescence microscopy in serum sickness nephritis induced with EA (Shigematsu and Koyama 1988a–c). The results, using an immunogold technique in the present study, show that EA, rat IgG and C3 are present in the Ds within the mesangial matrix and subepithelial region and the density of the Ds seems to represent the amount of the complexes of antigen and antibody. This is because the gold particle density is proportional to the electron density of the Ds. Further, the gold particles are mainly confined to Ds; thus the quantity of immune complex deposited in the glomerulus may be roughly reflected by the volume of Ds. Further, a quantitative analysis of the volume of Ds in different regions of glomerulus and different stages of the nephritis was carried out. The results confirm and extend previous observations (Thaiss et al. 1986; Sawtell et al. 1987; Fries et al. 1988) that the location of glomerular Ds is an important factor in determining the development of glomerular lesions and proteinuria. Ds are observed in both sides of GBM in some models (Koyama et al. 1978; Yamamoto et al. 1978; Sawtell et al. 1987, 1988; Shigematsu and Koyama 1988a–c), but in others Ds are only detected on the subepithelial

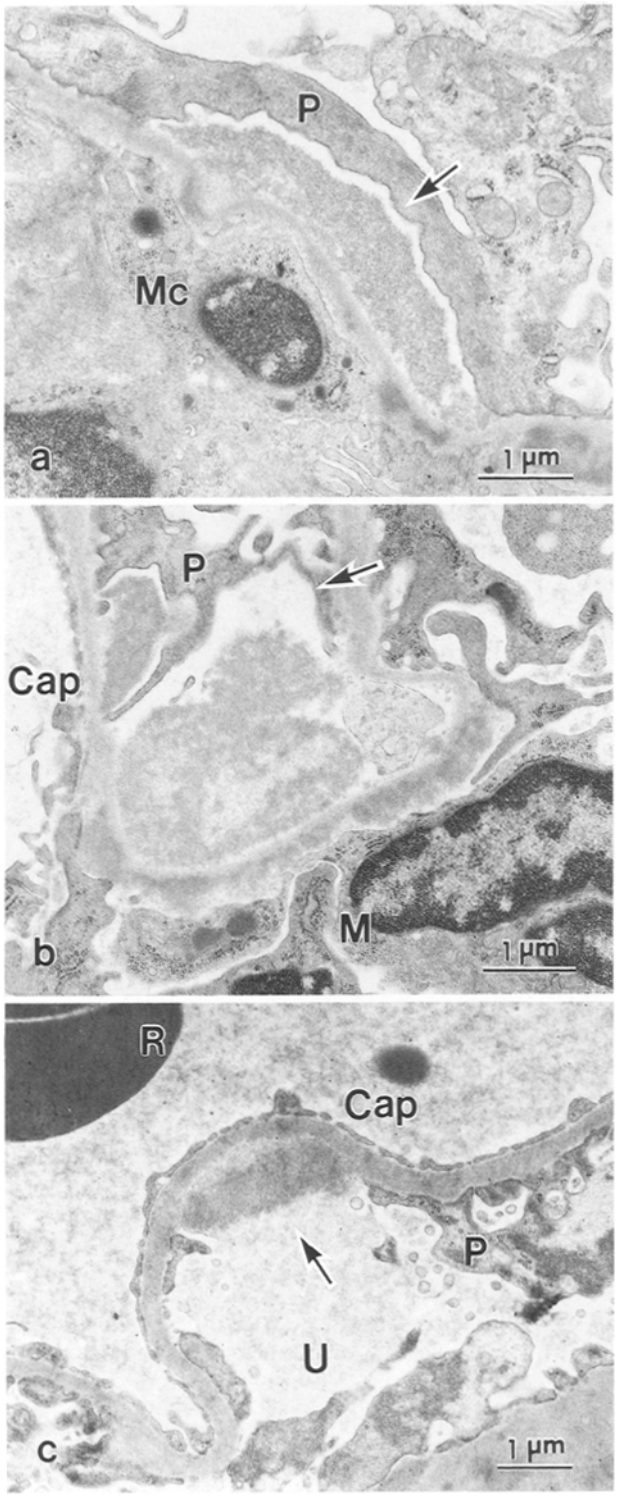

Fig. 10a–c. Electron micrographs showing that the large electron-dense deposits compress and lift the foot process, resulting in focal rupture of podocyte. *U*, Urinary space; *P*, podocyte; *Cap*, capillary lumen; *Mc*, mesangial cell; *M*, monocyte; *R*, red blood cell. **a** The lifting of podocytes overlying DPs and a gap can be seen (*arrow*). ×12500. **b** The lifting of podocytes is marked and the gap is wide (*arrow*). ×12000. **c** The wide rupture of podocytes exposes the electron-dense deposits to the urinary space (*arrow*). ×10250

side of GBM (Schneeberger et al. 1979; Adler et al. 1983). In these latter situations animals developed proteinuria. In contrast, animals with accumulation of Ds only on the subendothelial side did not develop proteinuria (Fries et al. 1988; Sawtell et al. 1988). In the present study, the rats without preimmunization showed only MDs and did not develop significant proteinuria. By quantitative analysis, it was found that the volume of PDs correlated with the amount of proteinuria, with loss of large molecular protein but the MDs did not correlate with the amount of proteinuria. This further suggests that the PDs, including the paramesangium, may be one of the factors involved in the development of proteinuria, whereas MDs are not, at least in this model. In addition, the PDs accumulating underneath the slit pores may more readily give rise to podocytic detachment, inducing proteinuria, than the PDs present underneath the foot processes.

The ultrafiltration unit of the glomerulus consists of endothelial fenestrae, GBM and epithelial foot processes with intervening slit diaphragms. Any damage to these structures may induce the abnormal loss of plasma protein into the urinary space (Kanwar 1984). The structural abnormalities of podocytes have been extensively examined in aminonucleoside nephrosis. The large balloon-like vacuoles (Venkatachalam et al. 1970; Messina et al. 1987) and detachment of podocytes (Ryan and Karnovsky 1975; Ryan et al. 1978; Olson et al. 1981; Kanwar and Rosenzweig 1982; Messina et al. 1987) are described, correlating well with the onset of proteinuria. However, the mechanism of proteinuria proposed in aminonucleoside nephrosis has been reported not to be applicable in serum sickness nephritis by Furness et al. (1989), who failed to find podocytic detachment in this model. However, the strain of rats and antigen they used and the length of injection of antigen were different from those in our study, and the deposition of immune complexes was not reported in detail.

In the present study, the widening of the slit and the loss of slit diaphragms were found at the time of onset of proteinuria. Definite epithelial detachment was found at 3 weeks when significant proteinuria and a number of large PDs appeared. In some areas, the slit diaphragms disappeared and the PDs were seen escaping into the subepithelial pockets or urinary space across the defects of the podocyte. In other areas, the epithelial foot processes have been partially lifted and detached from underlying PDs. Morphometric analysis indicated that the number of the sites of podocytic detachment correlates well with the urinary protein excretion rates. In addition, a tracer study using native ferritin showed that from the early stage of proteinuria the tracer molecules permeated full layers of GBM, but very few were seen in podocytes and the urinary space. However, in the rats with significant proteinuria, the tracer particles were detected in large amounts in the urinary space near the areas devoid of epithelial covering. Further, SDS-PAGE electrophoresis of urinary proteins indicated that the appearance of proteins with a molecular weight larger than 97000 daltons was clearly coincident with the development of podocytic detachment. From these

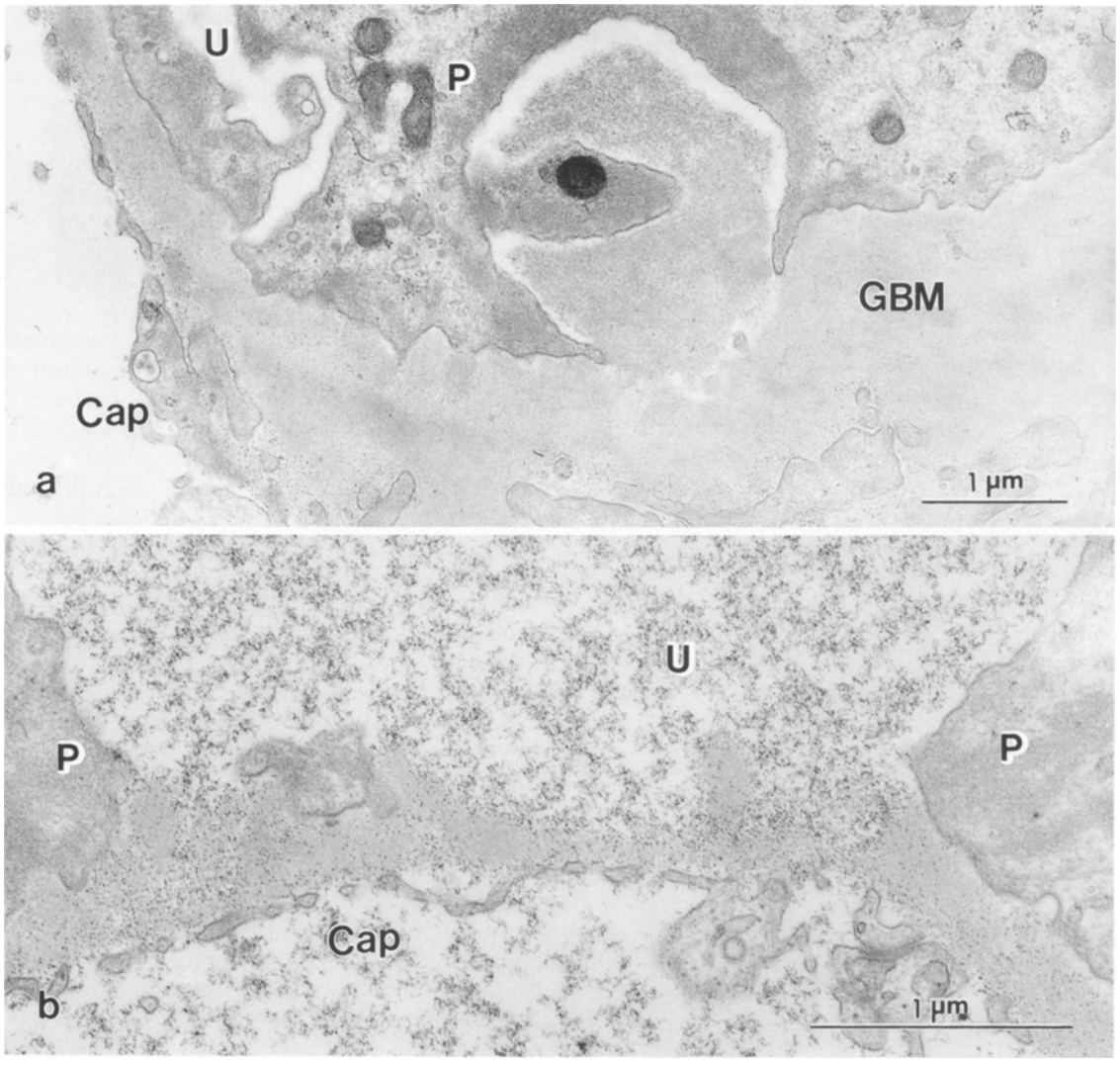

Fig. 11a, b. Distribution of native ferritin in glomeruli of proteinuric rats 4 weeks following intraperitoneal injection of EA. *U*, Urinary space; *P*, podocyte; *Cap*, capillary lumen; *GBM*, glomerular basement membrane. The detachment of podocytes from the GBM allows the passage of native ferritin into the subepithelial pocket (**a** ×20000) and the urinary space (**b** ×36500). Lead citrate stain

results it is suggested that from early stages of proteinuria the plasma proteins, regardless of size, had been allowed to cross the GBM, but only the proteins with a smaller molecular weight, such as albumin, could enter into the urinary space. The larger molecular proteins, such as gamma-globulin, could not reach the urinary space, because the podocytes were intact and the structural pores in the epithelial layer were smaller than those in the GBM (Ryan et al. 1976). Following the development of loss of slit diaphragms and detachment of podocytes, all of the plasma proteins, regardless of their size, were able to cross the GBM and the defect of podocytes into the urinary space. These data apparently support the finding that the loss of slit diaphragms and podocytic detachment from GBM are the significant events for the passage of plasma proteins (especially those with a larger molecular weight) across the capillary wall.

It is not clear by what mechanism the podocyte detaches from the GBM. In aminonucleoside nephrosis it has been proposed that puromycin aminonucleoside causes injury to podocytes which leads to a decrease in cell surface area and retraction of foot processes, leading to cellular separation from the GBM (Messina et al. 1987). Detachment of podocytes could also be due to a defect in the synthesis of either the basement membrane or podocyte surface components (Caulfield et al. 1976) or the disruption of a network of filaments which normally extend from the GBM to the adjoining cell surfaces (Kanwar and Farquhar 1980).

The loss of slit diaphragms (Adler et al. 1983) and detachment (Schneeberger et al. 1979) of podocytes covering PDs have been observed in some immune complex nephropathies. This study has shown that there are different patterns of production of podocytic lesions by the immune deposition in serum sickness nephritis. One is the interesting phenomenon where PDs pass across the defect of podocytes into the subepithelial pocket or urinary space, a change which has not previously been described. I think that the mechanism by which the podocyte detaches from the GBM in this model may be

different from that in aminonucleoside nephrosis. Podocytic lesions in this model may be described as follows, podocytic detachments were seen in the areas where large PDs existed and loss of slit diaphragms was observed beyond the accumulated PDs. Subepithelial pockets were seen to form following podocytic detachment and native ferritin injected in abdominal aorta evidently escaped into the urinary space through the sites of podocytic detachment. Electron-dense materials similar to PDs were found in the urinary space near the areas without epithelial covering. These observations impel me to propose the following two explanations for the development of podocytic detachment in this model.

Firstly, slit diaphragms might rupture due to the interposition of PDs underneath them. The loss of slit diaphragms may allow podocytes to retract in different directions, leaving areas without epithelial covering. The PDs pass through the defect of podocytes into the subepithelial pocket or into the urinary space. The PDs in the subepithelial pocket may also disrupt the overlying podocyte, as a result of the progressive accumulation of deposits and finally communicate with the urinary space. As an alternative hypothesis the large PDs situated beneath foot processes, often being flattened, could cause compression and lifting of the podocytic cytoplasm, resulting in separation of podocytes from the GBM forming a subepithelial pocket without continuity with the urinary space. With the increase of material in the pocket, some part of the podocytic cytoplasm might be broken and the material contained within would become exposed to the urinary space.

Data obtained recently using the deep-etching replica method also support my opinion that the accumulation of deposits in subepithelial regions is responsible for the podocytic detachment. The study of Nakazawa (in press) has disclosed that anchoring fibrils exist between the podocytic cell surface and lamina densa of GBM, and PDs have been shown to disrupt these fibrillar structures, resulting in partial podocytic detachment from the GBM.

The leakage of plasma proteins across the capillary wall at sites where podocytes have detached from GBM has been suggested as the result of focally increased bulk flow across these sites, since the epithelial layer exerts a significant influence upon water flux during ultrafiltration (Ryan and Karnovsky 1975, 1978; Kanwar and Rosenzweig 1982; Messina et al. 1987; Furness et al. 1989). If this is true it is not difficult to understand why the formation of PDs results in podocytic change leading to proteinuria. The large cytoplasmic vacuoles of podocytes have generally been considered to serve as the route for the transfer of proteins from the GBM to the urinary space in aminonucleoside nephrosis (Venkatachalam et al. 1970; Messina et al. 1987). They have been also observed in serum sickness nephritis (Furness et al. 1989). My quantitative results further confirm that the presence of these vacuoles correlates with the proteinuria in this model. However, whether this phenomenon represents the passage of plasma proteins across the epithelial layer, as is seen in aminonucleoside nephrosis, remains to be clarified.

From these results, it is suggested that podocytic damage including rupture of the slit diaphragm and detachment of foot processes from GBM due to the progressive accumulation of PDs will allow the leakage of plasma proteins across the capillary wall. This may be one of the main pathway of the heavy proteinuria in this model.

Acknowledgements. The author offers his grateful thanks to Prof. H. Shigematsu for fruitful instruction and helpful criticism of the manuscript, to Drs. K. Nakazawa, H. Ishigame, N. Itoh and N. Yamaguchi for assistance in this study. The assistance provided by Dr. S. Sun in the SDS-PAGE electrophoresis and the technical assistance of Miss T. Nishizawa, Miss N. Aoshima, Mrs. M. Watanabe, Mr. R. Ichikawa and Mr. K. Kametani are grateful acknowledged.

References

Adler S, Salant DJ, Dittmer JE, Rennke HG, Madaio MP, Couser WG (1983) Mediation of proteinuria in membranous nephropathy due to a planted glomerular antigen. Kidney Int 23:807–815

Bendayan M, Zollinger M (1983) Ultrastructural localization of antigenic sites on osmium-fixed tissues applying the protein A-gold technique. J Histochem Cytochem 31:101–109

Caulfield JP, Reid JJ, Farquhar MG (1976) Alterations of glomerular epithelium in acute aminonucleoside nephrosis: evidence for formation of occluding junctions and epithelial detachment. Lab Invest 34:43–59

Fraij BM (1989) Separation and identification of urinary proteins and stone-matrix proteins by mini-slab sodium dodecyl sulfate-polyacrylamide gel electrophoresis. Clin Chem 35:658–662

Fries JWU, Mendrick DL, Rennke HG (1988) Determinants of immune complex-mediated glomerulonephritis. Kidney Int 34:333–345

Furness PN, Turner SN, Appleby P, Turner DR (1989) A morphological study of experimental proteinuria using a novel form of surface fixation. J Pathol 157:37–45

Hearn SA, Silver MM, Sholdice JA (1985) Immunoelectron microscopic labeling of immunoglobulin in plasma cells after osmium fixation and epoxy embedding. J Histochem Cytochem 33:1212–1218

Kanwar YS (1984) Biology of disease. Biophysiology of glomerular filtration and proteinuria. Lab Invest 51:7–21

Kanwar YS, Farquhar MG (1980) Detachment of endothelium and epithelium from the glomerular basement membrane produced by kidney perfusion with neuraminidase. Lab Invest 42:375–384

Kanwar YS, Rosenzweig LJ (1982) Altered glomerular permeability as a result of focal detachment of visceral epithelium. Kidney Int 21:565–574

Kelley VE, Cavallo T (1977) Glomerular permeability. Ultrastructural studies in New Zealand Black/White mice using polyanionic ferritin as a molecular probe. Lab Invest 37:265–275

Kelley VE, Cavallo T (1978) Glomerular permeability. Transfer of native ferritin in glomeruli with decreased anionic sites. Lab Invest 39:547–553

Kelley VE, Cavallo T (1980) Glomerular permeability. Focal loss of anionic sites in glomeruli of proteinuric mice with lupus nephritis. Lab Invest 42:59–64

Koyama A, Niwa Y, Shigematsu H, Taniguchi M, Tada T (1978) Studies on passive serum sickness. II. Factors determining the localization of antigen-antibody complexes in the murine renal glomerulus. Lab Invest 38:253–262

Laemmli UK (1970) Cleavage of structural proteins during the assembly of the head of bacteriophage T4. Nature 227:680–685

McCluskey RT (1983) Immunologic mechanisms in glomerular dis-

ease. In: Heptinstall RH (ed) Pathology of kidney. Little Brown, Boston, pp 301–386

Messina A, Davies DJ, Dillane PC, Ryan GB (1987) Glomerular epithelial abnormalities associated with the onset of proteinuria in aminonucleoside nephrosis. Am J Pathol 126:220–229

Olson JL, Rennke HG, Venkatachalam MA (1981) Alterations in the charge and size selectivity barrier of the glomerular filter in aminonucleoside nephrosis in rats. Lab Invest 44:271–279

Ryan GB, Karnovsky MJ (1975) An ultrastructural study of the mechanisms of proteinuria in aminonucleoside nephrosis. Kidney Int 8:219–232

Ryan GB, Leventhal M, Karnovsky MJ (1975a) A freeze-fracture study of the junctions between glomerular epithelial cells in aminonucleoside nephrosis. Lab Invest 32:397–403

Ryan GB, Rodewald R, Karnovsky MJ (1975b) An ultrastructural study of the glomerular slit diaphragm in aminonucleoside nephrosis. Lab Invest 33:461–468

Ryan GB, Hein SJ, Karnovsky MJ (1976) Glomerular permeability to proteins. Effects of hemodynamic factors on the distribution of endogenous immunoglobulin G and exogenous catalase in the rat glomerulus. Lab Invest 34:415–427

Ryan GB, Hein SJ, Karnovsky MJ (1978) The distribution of albumin and immunoglobulin G in the glomerular capillary wall in aminonucleoside nephrosis. Pathology 10:335–341

Sawtell NM, Weiss MA, Pesce AJ, Michael JG (1987) An immune complex glomerulopathy associated with glomerular capillary thrombosis in the laboratory mouse: a highly reproducible accelerated model utilizing cationized antigen. Lab Invest 56:256–263

Sawtell NM, Hartman AL, Weiss MA, Pesce AJ, Michael JG (1988) C3 dependent, C5 independent immune complex glomerulopathy in the mouse. Lab Invest 58:287–293

Schneeberger EE, O'Brien A, Grupe WE (1979) Altered glomerular permeability in Munich-Wistar rats with autologous immune complex nephritis. Lab Invest 40:227–235

Shigematsu H, Koyama A (1988a) Suppressive effect of cyclosporin A on the induction of chronic serum sickness nephritis in the rat. Acta Pathol Jpn 38:11–19

Shigematsu H, Koyama A (1988b) Therapeutic effect of cyclosporin A and steroid on serum sickness type nephritis in the rat. I. Suppression of the antibody response and induction of glomerulonephritis. Jpn J Nephrol 30:1109–1114

Shigematsu H, Koyama A (1988c) Therapeutic effect of cyclosporin A and steroid on serum sickness type nephritis in the rat. II. Suppressive effect on full-blown proliferative glomerulonephritis. Jpn J Nephrol 30:1115–1122

Thaiss F, Batsford S, Mihatsch MJ, Heitz PU, Biter-Suermann D, Vogt A (1986) Mediator systems in a passive model of in situ immune complex glomerulonephritis: role for complement, polymorphonuclear granulocytes and monocytes. Lab Invest 54:624–635

Venkatachalam MA, Cotran RS, Karnovsky MJ (1970) An ultrastructural study of glomerular permeability in aminonucleoside nephrosis using catalase as a tracer protein. J Exp Med 132:1168–1180

Yamamoto T, Kihara I, Morita T, Oite T (1978) Bovine serum albumin (BSA) nephritis in rats. I. Experimental model. Acta Pathol Jpn 28:859–866